(3) Simionescu, C. I.; Simionescu, B. C.; Leanca, M.; Ananiescu, C. *Polym. Bull. (Berlin)* **1981**, *5*, 61.
(4) Simionescu, B. C.; Popa, M.; Ioan, S.; Simionescu, C. I. *Polym. Bull. (Berlin)* **1982**, *6*, 415.
(5) Kashiwagi, Y.; Einaga, H.; Fujita, H. *Polym. J. (Tokyo)* **1980**, *12* (4), 271.
(6) Simionescu, B. C.; Ioan, S.; Simionescu, C. I. *Polym. Bull. (Berlin)* **1982**, *6*, 409.
(7) Ioan, S.; Simionescu, B. C.; Simionescu, C. I. *Polym. Bull. (Berlin)* **1982**, *6*, 421.
(8) Johnson, D. R.; Osada, Y.; Bell, A. T.; Shen, M. *Macromolecules* **1981**, *14*, 118.
(9) Simionescu, B. C.; Natansohn, A.; Simionescu, C. I. *Polym. Bull. (Berlin)* **1980**, *2*, 809.
(10) Simionescu, B. C.; Natansohn, A.; Leanca, M.; Ananiescu, C.; Simionescu, C. I. *Polym. Bull. (Berlin)* **1980**, *3*, 247.
(11) Simionescu, B. C.; Natasohn, A.; Leanca, M.; Ananiescu, C.; Simionescu, C. I. *Polym. Bull. (Berlin)* **1981**, *4*, 569.
(12) Paul, C. W.; Bell, A. T.; Soong, D. S. *Macromolecules*, preceding paper in this issue.
(13) Naylor, M. A.; Billmeyer, F. W., Jr. *J. Am. Chem. Soc.* **1953**, *75*, 2181.
(14) Pulley, J. M.S. Thesis, Rensselaer Polytechnic Institute, Troy, NY, 1969.
(15) Chinai, S. N.; Matlack, J. D.; Resnick, A. L.; Samuels, R. J. *J. Polym. Sci.* **1955**, *17*, 391.
(16) Bevington, J. C.; Melville, H. W.; Taylor, R. P. *J. Polym. Sci.* **1954**, *14*, 463.
(17) Brandrup, J., Immergut, E. H., Eds. "Polymer Handbook"; Wiley: New York, 1975.
(18) Stickler, M.; Meyerhoff, G. *Makromol. Chem.* **1978**, *179*, 2729.
(19) Paul, C. W.; Bell, A. T.; Soong, D. S. Part 3 of this series, to be submitted.
(20) Balke, S. T.; Hamielec, A. E. *J. Appl. Polym. Sci.* **1973**, *17*, 905.
(21) Flory, P. J. "Principles of Polymer Chemistry"; Cornell University Press: Ithaca, NY, 1953.
(22) Bristow, G. M.; Watson, W. F. *Trans. Faraday Soc.* **1958**, *54*, 1742.
(23) Schulz, G. V.; Baumann, H.; Daiskus, R. *J. Phys. Chem.* **1966**, *70*, 3647.

Reversible Singlet Energy Transfer in 1,3-Di(2-naphthyl)propyl Acetate

J. Vandendriessche, P. Collart, and F. C. De Schryver*

Department of Chemistry, University of Leuven, Celestijnenlaan 200 F, B-3030 Heverlee, Belgium

Q. F. Zhou and H. J. Xu

Institute of Photographic Chemistry, Academia Sinica, Bei Sha Tan, Beijing, The People's Republic of China.

Received March 11, 1985

ABSTRACT: The photophysical properties of 1,3-di(2-naphthyl)propyl acetate at low temperatures (253-213 K) in isooctane were investigated. Fluorescence lifetime measurements revealed the existence of two excimers and reversible singlet energy transfer. The rate constant of singlet energy transfer from the methylene-substituted naphthalene to the naphthalene next to the acetate group equals 1.3×10^9 ($\pm 7 \times 10^8$) s^{-1}. The rate of the reverse process equals 2.7×10^9 ($\pm 1.5 \times 10^9$) s^{-1}.

Introduction

Intramolecular excimer formation in molecules containing two or more naphthalene chromophores has been the subject of active research since the first observations by Vala et al.[1] and has been reviewed recently.[2] Although previously only one excimer fluorescence peak and decay were observed for R-CHX-Z-CHY-R, where R = 1-naphthyl or 2-naphthyl, X, Y = H or methyl, and Z = CH_2,[3] recent results based on fluorescence decay measurements indicate more complex kinetics.[4,5] The analysis of the decay parameters measured in the excimer region as well for 1,3-di(1-naphthyl)propane in methylene chloride, for 1,3-di(2-naphthyl)propane in tetrahydrofuran and methylene chloride,[4] for *meso*-bis[1-(2-naphthyl)ethyl] ether in isooctane, and for bis(1-naphthylmethyl) ether[5] confirms the presence of more than one excimer species. The photophysical properties of poly(1-vinylnaphthalene) and poly(2-vinylnaphthalene) were shown to be complex.[5,6] Whether electronic energy migration between the chromophores of the polymer in solution occurs is still a point of discussion.[2]

To gain some insight into this problem the photophysical properties of 1,3-di(2-naphthyl)propyl acetate (DNPA) (R = 2-naphthyl, X = H, Y = $OCOCH_3$, Z = CH_2) were investigated. The introduction of an acetate group influences the radiative and nonradiative decay processes of the naphthalene chromophore next to the acetate group. The process of reversible singlet energy transfer becomes thus detectable with a fluorescence lifetime apparatus.

Experimental Section

Fluorescence spectra and quantum yields were obtained with a computerized Spex Fluorolog 1902 using double monochromators in both excitation and emission. Quantum yields were determined by using quinine sulfate in 0.1 N H_2SO_4 ($\Phi_f = 0.545$)[7] as standard. Correction for the refractive index of the solvents was applied. The optical densities were measured with a Perkin-Elmer Lamba 5 UV-vis spectrophotometer. The absorbances at the excitation wavelength were less than 0.1. Fluorescence decays were measured with a Spectra Physics frequency-doubled cavity-dumped mode-locked synchronously pumped R6G dye-laser system with time-correlated single-photon-counting detection. The fluorescence lifetime apparatus, the associated optical and electronic components, and data analysis are described in detail elsewhere.[8]

1,3-Di(2-naphthyl)propyl acetate (DNPA), (2-naphthyl)methyl acetate (NMA), and 2-methylnaphthalene (MN) are the same as used before and of HPLC controlled purity.[9] Isooctane (Merck for fluorimetry) was purified over a column with silica gel and carbon black. No fluorescence could be detected from the purified solvent under the excitation conditions used in this work. The solutions were deareated by the freeze-pump-thaw method (typically 4 cycles). The temperature of the sample was kept constant by circulating nitrogen through the cell holder. The temperature stability was better than 1 K.

Results

Absorption Spectra. The positions of the absorption maxima in the absorption spectrum of NMA and in the absorption spectrum of MN are identical in the 240-300-nm region (^1L_a) but different in the 300-450-nm region (^1L_b) (Figure 1). The experimentally determined molar

0024-9297/85/2218-2321$01.50/0

Table I
Decay[a] and Fitting[b] Parameters of 1,3-Di(2-naphthyl)propyl Acetate in Isooctane[c]

T, K	λ_{em},[d] nm	A_1	τ_1, ns	A_2	τ_2, ns	A_3	τ_3, ns	χ^2	Z_{χ^2}	DW
253	330	0.39	0.20	0.97	6.19			1.12	−1.31	2.07
253[e]	330	2.01	6.04					2.32	14.60	1.02
243	330	0.19	0.28	0.95	8.10			1.28	−3.89	1.78
233	330	0.15	0.31	0.92	10.45			1.19	−3.25	1.79
223	330	0.31	0.21	0.95	13.65			1.15	−1.55	2.02
213	330	0.30	0.15	0.98	17.57			1.07	0.95	2.18
253	440	−1.16	6.77	0.76	43.99	0.59	121.3	1.10	0.56	2.11
243	440	−1.16	9.24	0.84	51.53	0.50	127.5	1.04	0.37	2.15
233	440	−1.02	11.33	0.70	54.21	0.46	123.1	1.05	0.53	2.18
223	440	−1.93	15.76	1.14	48.93	0.95	114.6	1.15	−1.95	2.17
213	440	−1.31	20.14	1.07	65.39	0.38	136.7	1.01	0.00	2.04

[a] Decay curves fitted to functions containing one, two, or three exponential decaying terms: $I(t) = \sum A_i \exp(-t/\tau_i)$. [b] For meaning of χ^2, Z_{χ^2}, and DW see ref 8 and references cited therein. [c] λ_{ex} = 293 nm; channel increment: 0.035 ns. [d] 330 nm corresponds to monomer region, 440 nm to excimer region. [e] Same curve fitted with a one-exponential trial function.

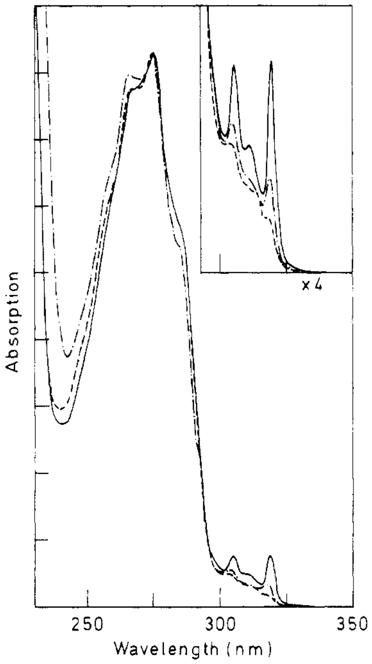

Figure 1. Absorption spectra of 2-methylnaphthalene (MN) (—), (2-naphthyl)methyl acetate (NMA) (- - -), and 1,3-di(2-naphthyl)propyl acetate (DNPA) in isooctane at 293 K (-·-). [MN] = [NMA] = $^1/_2$[DNPA].

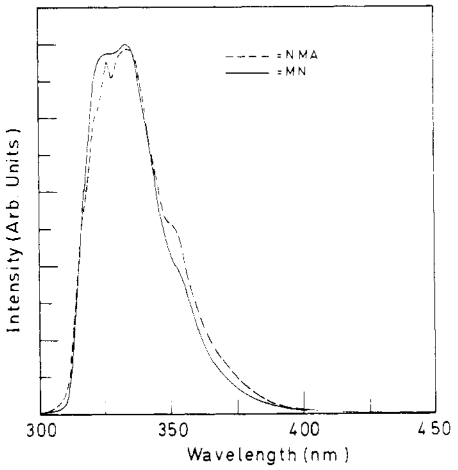

Figure 2. Fluorescence spectra of 2-methylnaphthalene in isooctane at 253 K (—) and (2-naphthyl)methyl acetate in isooctane at 253 K (- - -). λ_{ex} = 280 nm.

Scheme I
Kinetic Scheme for the Interpretation of the Photophysical Properties of 1,3-Di(2-naphthyl)propyl Acetate

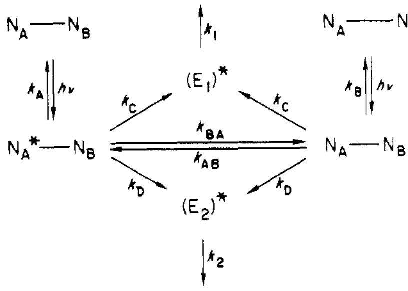

extinction coefficient of NMA at 274 nm equals 5400; this is, within experiment error, the same as reported for MN.[10] The extinction coefficients of NMA in the 300–350-nm region differ even up to $^1/_4$ of the extinction coefficient of MN. The absorption spectrum of DNPA equals the sum of the absorption spectra of NMA and MN; hence no important ground-state interaction between the chromophores in DNPA is detected.

Fluorescence Spectra. The fluorescence spectra of DNPA in methylcyclohexane as a function of temperature from 193 to 243 K are reported elsewhere.[9] Besides locally excited-state emission, excimer emission is observed with a maximum at 395 nm. For the reported temperature region an isoemissive point is detected at 372 nm. The fluorescence spectra of NMA and MN in isooctane at 253 K are shown in Figure 2. The position of the emission maxima is identical but differences in relative intensities of the peaks are observed. The quantum yield of emission of NMA and MN equals 0.24 and 0.27, respectively.

Fluorescence Decays. The emission of MN in isooctane, monitored at 330 nm, decays monoexponentially at all temperatures. The lifetime varies from 60.6 ns at 253 K to 66.5 ns at 193 K. The emission of NMA in isooctane, monitored at 330 nm, decays monoexponentially at all temperatures. The lifetime varies from 47.9 ns at 253 K to 52.0 ns at 193 K.

The emission decay of DNPA in isooctane, monitored at 330 nm, can be described adequately by a sum of two exponential terms at all temperatures below 253 K (Table I). The emission decay of DNPA in isooctane, monitored at 440 nm, can be analyzed as a three-exponential function in the same temperature region. One of the exponential terms has a negative preexponential factor (Table I).

Discussion

For the interpretation of the experimental data Scheme I was developed. In Scheme I N_A represents the naphthalene chromophore with CH_2 as substituent and N_B represents the naphthalene chromophore next to the $OCOCH_3$ group. k_A equals the sum of radiative and nonradiative rate constants for processes from the locally excited N_A state; in the analysis the rate constants of radiative and nonradiative processes from MN were used. k_B equals the sum of radiative and nonradiative rate constants for processes from the locally excited N_B state; NMA served as a model. k_C and k_D are the rate constants of excimer formation of E_1 and E_2, respectively. It is assumed that the rate constant for excimer formation from the locally excited N_A state is the same as the rate constant for excimer formation from the locally excited N_B state. This assumption can be made since the chain rotation leading to the given excimer conformation is identical for N_A^*–N_B and N_A–N_B^*. k_1 and k_2 are the sum of radiative and nonradiative decay constants from E_1 and E_2, respectively. k_{BA} is the rate constant of energy transfer from the locally excited N_A state to N_B. k_{AB} is the rate constant of energy transfer from the locally excited N_B state to N_A. In Scheme I it is also assumed that there is no slow conformational preequilibrium;[3c,11] i.e., excimer formation occurs from a "pool" of rapidly equilibrating conformations represented by N_A–N_B.

The existence of two excimers in DNPA can be understood in analogy with the situation found for *meso*-2,4-di(1-pyrenyl)pentane[12] and 1,3-di(1-pyrenyl)propane.[13] Furthermore, the measurements reported in the present report were performed at temperatures where back-dissociation of the excimers can be neglected.

The theoretical decay functions of N_A^*, N_B^*, and the excimers are derived analogously to the method used in the literature.[14] The derivation of the equations is straightforward and thus not given in detail. The following equations for the concentration dependence of the excited states as a function of time (t) result:

$$[N_A^*]_t = C_1 \exp(-\lambda_1 t) + C_2 \exp(-\lambda_2 t) \quad (1)$$

$$[N_B^*]_t = C_3 \exp(-\lambda_1 t) + C_4 \exp(-\lambda_2 t) \quad (2)$$

$$[E_1]_t = C_5 \exp(-\lambda_1 t) + C_6 \exp(-\lambda_2 t) + C_7 \exp(-\lambda_3 t) \quad (3)$$

$$[E_2]_t = C_8 \exp(-\lambda_1 t) + C_9 \exp(-\lambda_2 t) + C_{10} \exp(-\lambda_4 t) \quad (4)$$

where

$$\lambda_{1,2} = \tfrac{1}{2}(k_A' + k_B' \pm [(k_A' - k_B')^2 + 4k_{AB}k_{BA}]^{1/2}) \quad (5)$$

$$\lambda_3 = k_1 \quad (6)$$

$$\lambda_4 = k_2 \quad (7)$$

$$k_A' = k_A + k_C + k_D + k_{BA} \quad (8)$$

$$k_B' = k_B + k_C + k_D + k_{AB} \quad (9)$$

$$C_1 = [N_A^*]_0(k_A' - k_{AB} - \lambda_2)/(\lambda_1 - \lambda_2)$$

$$C_2 = [N_A^*]_0(\lambda_1 - k_A' + k_{AB})/(\lambda_1 - \lambda_2)$$

$$C_3 = [N_B^*]_0(k_B' - k_{BA} - \lambda_2)/(\lambda_1 - \lambda_2)$$

$$C_4 = [N_B^*]_0(\lambda_1 - k_B' + k_{BA})/(\lambda_1 - \lambda_2)$$

$$C_5 = k_C(C_1 + C_3)/(k_1 - \lambda_1)$$

$$C_6 = k_C(C_2 + C_4)/(k_1 - \lambda_2)$$

$$C_7 = -(C_5 + C_6)$$

$$C_8 = k_D(C_1 + C_3)/(k_2 - \lambda_1)$$

$$C_9 = k_D(C_2 + C_4)/(k_2 - \lambda_2)$$

$$C_{10} = -(C_8 + C_9)$$

and $[N_A^*]_0$ and $[N_B^*]_0$ are the concentrations of N_A and N_B in the excited state at time zero. In this derivation an equal probability of excitation is assumed. This assumption is justifiable since the molar extinction coefficients of MN and NMA at the wavelength of excitation (293 nm) are equal within experimental error. The fluorescence decay at 330 nm, the wavelength of monomer emission analysis, is the sum of the decays of N_A^* and N_B^*. With

$$i_{N_A}(t) = k_{FA}[N_A^*]/[N_A^*]_0$$

$$i_{N_B}(t) = k_{FB}[N_B^*]/[N_B^*]_0$$

where k_{FA} and k_{FB} are the rate constants of radiative decay of N_A^* and N_B^*, respectively, we obtain

$$i_{N_A+N_B}(t) = \frac{k_{FA}(k_A' - k_{AB} - \lambda_2) + k_{FB}(k_B' - k_{BA} - \lambda_2)}{\lambda_1 - \lambda_2} \exp(-\lambda_1 t) + \frac{k_{FA}(\lambda_1 - k_A' + k_{AB}) + k_{FB}(\lambda_1 - k_B + k_{BA})}{\lambda_1 - \lambda_2} \exp(-\lambda_2 t) \quad (10)$$

The fluorescence decay in the monomer region is thus the sum of two exponentials. It is easily seen that if k_{AB}, $k_{BA} \gg k_A + k_C + k_D$, $k_B + k_C + k_D$, a single exponential results with $\lambda_2 = (k_A + k_B)/2 + k_C + k_D$. λ_1 becomes very large and the preexponential term of $-\lambda_1 t$ very small: the contribution of λ_1 to the decay when k_{AB}, $k_{BA} = 10^{10}$ s^{-1} equals $\pm 10^{-7}$%. If k_{AB}, $k_{BA} \ll k_A + k_C + k_D$, $k_B + k_C + k_D$, a two-exponential function results with $\lambda_1 = k_A'$ and $\lambda_2 = k_B'$. Between these two situations a two exponential will be observed with a short decaying component which contributes less than the long-decaying component.

The fluorescence decay at 440 nm, the wavelength of excimer emission analysis, is the sum of the decays of E_1 and E_2 under the assumption that the emission spectra of both excimers are identical. A four-exponential function results. Further elaboration of this decay function is, in view of the aim of this article, not relevant.

Before an analysis of the fitting parameters was performed, two questions had to be solved. Is the data analysis used able to resolve a two-exponential decay from data that contain an equal contribution of two decays in a ratio 47.9/60.6? Can a two-exponential decay curve be analyzed adequately when one of the decays is very short (0.2 vs. 20 ns) and contributes little to the total emission (~1%)? An answer to these questions was obtained with a simulation program that generates decay curves. Details of this simulation technique will be reported separately.[15] For a ratio of 47.9/60.6 $(k_B + k_C + k_D)/(k_A + k_C + k_D)$ a two-exponential decay should be observed, but good fits were also obtained when a one-exponential trial function was used. From this we concluded that if energy transfer is unimportant (k_{AB}, $k_{BA} \ll k_A + k_C + k_D$, $k_B + k_C + k_D$) we should have found good fits for the one-exponential fitting of the experimentally obtained decays at 330 nm. This is not the case (Table I). On the other hand, the simulation procedure proved that fitting of decays with a short-decaying component with little contribution is possible and adequate. Analysis of the data reported in Table I is further used to obtain an idea about the magnitude of the energy rate constants k_{AB} and k_{BA} as follows. Since $\lambda_1 > \lambda_2$ ($\lambda_i = 1/\tau_i$) it is concluded that k_{AB}, $k_{BA} > k_A + k_C + k_D$, $k_B + k_C + k_D$. According to eq 5, $\lambda_1 \approx k_{AB} + k_{BA}$. This sum is independent of temperature and equals 4×10^9 ($\pm 1.5 \times 10^9$) s^{-1}. It is not possible to obtain accurate values for k_{AB} and k_{BA} separately. At the distances where the two chromophores are situated upon excitation and during the excimer formation process, singlet energy transfer can occur by more than one mechanism: a ratio of k_{AB}/k_{BA} obtained from the ratio of the spectral overlap integrals ($k_{AB}/k_{BA} = 3$ using equations of Förster;[16] $k_{AB}/k_{BA} = 1.5$ using equations of Dexter[17]) can thus not serve as a second independent equation relating k_{AB} and k_{BA}. The ratios of the overlap integrals however give an idea about the magnitude of k_{AB} and k_{BA}. k_{AB} is estimated to be 2.7 × 10^9 (±1.5 × 10^9) s^{-1} and k_{BA} 1.3 × 10^9 (±7 × 10^8) s^{-1}.

The good fits (Table I) obtained in the excimer region are understood when one takes into account the low contribution of λ_1 in eq 3 and 4 and the fact that these results are fitted with seven variables.[18]

The analysis of DNPA makes clear the importance of reversible singlet energy transfer in excimer-forming molecules. It proves the importance of intramolecular singlet energy transfer and energy migration in molecules containing two or more chromophores in solution. The process of reversible energy transfer or migration will only show up kinetically when two chromophores involved have slightly different photophysical properties.

Acknowledgment. This research was supported in part by grants from the University Research Fund and the FKFO. Q.F.Z. thanks the National Science Foundation and the Academia Sinica for permission to take part in an exchange program allowing him to stay at the University of Leuven. J.V. and P.C. are grateful to the IWONL for a predoctoral fellowship. We thank Dr. N. Boens for the development of data analysis and simulation programs.

References and Notes

(1) Vala, M. T.; Haebig, J.; Rice, S. A. *J. Chem. Phys.* **1965**, *43*, 886.

(2) Semerak, S. N.; Frank, C. W. *Adv. Polym. Sci.* **1984**, *54*, 31.

(3) (a) Chandross, E. A.; Dempster, C. J. *J. Am. Chem. Soc.* **1970**, *92*, 3586. (b) Avouris, P.; Kordas, J.; El-Bayoumi, M. A. *Chem. Phys. Lett.* **1974**, *26*, 373. (c) Goldenberg, M.; Emert, J.; Morawetz, H. *J. Am. Chem. Soc.* **1978**, *100*, 7171. (d) Ito, S.; Yamamoto, M.; Nishijima, Y. *Bull. Chem. Soc. Jpn.* **1981**, *54*, 35.

(4) Phillips, D.; Rumbles, G. *Polym. Photochem.* **1984**, *5*, 153.

(5) (a) Demeyer, K.; Van der Auweraer, M.; Aerts, L.; De Schryver, F. C. *J. Chim. Phys. Phys.-Chim. Biol.* **1980**, *77*, 493. (b) De Schryver, F. C.; Demeyer, K.; Van der Auweraer, M.; Quanten, E. *Ann. N.Y. Acad. Sci.* **1981**, *366*, 93. (c) Todesco, R.; Gelan, J.; Martens, H.; Put, J.; De Schryver, F. C. *J. Am. Chem. Soc.* **1981**, *103*, 7304.

(6) Phillips, D.; Roberts, A. J.; Soutar, I. *J. Polym. Sci., Polym. Phys. Ed.* **1982**, *20*, 411.

(7) Demas, J. N.; Crosby, G. A. *J. Phys. Chem.* **1971**, *75*, 991. Morris, J. V.; Mahaney, M. A.; Huber, J. R. *J. Phys. Chem.* **1976**, *80*, 969.

(8) Boens, N.; Van den Zegel, M.; De Schryver, F. C. *Chem. Phys. Lett.* **1984**, *111*, 340.

(9) (a) Xu, H. J.; Yas, S. M.; Shen, S. Y.; Yang, Z. X.; Zhang, H.; Zhou, Q. F.; Ma, G. J. *Acta Chim. Sin.* **1982**, *40*, 803. (b) Xu, H. J.; Shou, H. S.; Shen, S. Y.; Zhou, Q. F. *Acta Chim. Sin.* **1984**, *42*, 277.

(10) Berlman, I. B. In "Handbook of Fluorescence Spectra of Aromatic Molecules", 2nd ed.; Academic Press: New York, 1971; p 333.

(11) Vandendriessche, J.; Palmans, P.; Toppet, S.; Boens, N.; De Schryver, F. C.; Masuhara, H. *J. Am. Chem. Soc.* **1984**, *106*, 8057.

(12) Collart, P.; Toppet, S.; Zhou, Q. F.; Boens, N.; De Schryver, F. C. *Macromolecules* **1985**, *18*, 1026.

(13) Zachariasse, K. A.; Busse, R.; Duvenek, G.; Kühnle, W. Proceedings of the Xth IUPAC Symposium on Photochemistry, 1984, p 47.

(14) (a) Birks, J. B. In "Photophysics of Aromatic Molecules"; Wiley-Interscience: New York, 1970. (b) Itagaki, H.; Obukata, N.; Okamoto, A.; Horie, K.; Mita, I. *J. Am. Chem. Soc.* **1982**, *104*, 4469. (c) Goedeweeck, R.; Van der Auweraer, M.; De Schryver, F. C. *J. Am. Chem. Soc.* **1985**, *107*, 2334.

(15) Boens, N.; Desie, G.; Van den Zegel, M.; De Schryver, F. C., to be published.

(16) Förster, Th., *Ann. Phys.* **1948**, *2*, 55; *Z. Naturforsch.* **1949**, *49*, 321; *Z. Elektrochem.* **1949**, *53*, 93.

(17) Dexter, D. L. *J. Chem. Phys.* **1953**, *21*, 836.

(18) Van der Auweraer, M.; Van den Zegel, M.; Boens, N.; De Schryver, F. C.; Willig, F., in press.

Notes

Kerr Effect and Dielectric Study of Poly(vinyl bromide) Oligomers

ALAN E. TONELLI,* GARO KHANARIAN,[†] and
RUDOLF E. CAIS

AT&T Bell Laboratories, Murray Hill,
New Jersey 07974. Received December 27, 1984

Recently two rotational isomeric states (RIS) models have been derived to describe the conformational characteristics of poly(vinyl bromide) (PVB). Tonelli[1] estimated the conformational energies for the chain segments found in PVB and the copolymers (PEVB) of vinyl bromide (VB) with ethylene (E). RIS models for PVB and PEVB were derived from these energy estimates, where both comonomer sequence and VB stereosequence were considered. Saiz et al.[2] also performed energy estimates on PVB segments and derived an RIS model for PVB. In addition, they measured the dipole moments of atactic PVB in two solvents (*p*-dioxane and 1-methylnaphthalene).

Both conformational descriptions, RIS-T (Tonelli[1]) and RIS-S (Saiz et al.[2]), reproduce the experimentally observed[2] dipole moments of atactic PVB ($C_m = \langle\mu^2\rangle/xm^2$ = 0.45–0.53, where x is the degree of polymerization and m is the C–Br bond dipole moment), yielding C_m = 0.41 (RIS-T) and C_m = 0.57 (RIS-S). In addition, the dimensions $C_r = \langle r^2\rangle_0/nl^2$, where $n = 2x$ and l is the length of a C–C bond, reported for atactic PVB by Ciferri and Lauretti[3] (C_r = 6.6) also agree with those predicted by RIS-T (5.3–5.7) and RIS-S (7.3–6.9) (see Table I).

Table I
Comparison of Calculated and Observed Dipole Moments and Dimensions for Atactic PVB

method	$C_m{}^a = \langle\mu^2\rangle/xm^2$	$C_r{}^b = \langle r^2\rangle_0/nl^2$
expt[2,3]	0.45–0.53	6.6
RIS-T[1]	0.41	5.3–5.7
RIS-S[2]	0.57	7.3–6.9

[a] For atactic[2] PVB with P_m = 0.46. [b] For atactic[1-4] PVB with P_m = 0.4–0.6.

Despite the apparent agreement between the dipole moments (C_m) and dimensions (C_r) observed for atactic PVB and the values obtained with either RIS-T or RIS-S, there are differences between the two conformational descriptions. Both RIS models find the tg and gt conformations to be preferred for meso (m) PVB diads, albiet to different degrees. Though both RIS models find the tt and gg conformers to be preferred for racemic (r) dyads, RIS-T predicts the gg conformer to be preferred over the tt conformer, while the tt conformer is preferred over the gg conformer in the RIS-S description.

[†] Present address: Celanese Research Co., Summit, NJ 07901.

0024-9297/85/2218-2324$01.50/0